基于小波变换的 MAG 快速成形焊缝截面建模

曹 勇，朱 胜，孙 磊，王望龙
（装甲兵工程学院 装备再制造技术国防科技重点实验室，北京 100072）

曹 勇

摘 要：提出一种基于小波变换的焊缝截面形态建模方法。基于小波变换模极大原理提取了典型焊缝截面轮廓，分别采用三次样条、带约束的三次样条以及 B 样条曲线方法对提取的焊缝轮廓进行插值，并基于最小二乘法对插值后的焊缝边缘轮廓进行了数据拟合，得到了焊缝轮廓数学模型。结果表明，采用小波变换提取焊缝截面轮廓是可行的，带约束的三次样条曲线过渡平滑、无突变点，在该试验条件下得到的焊缝截面轮廓数学模型为正弦曲线。

关键词：快速成形；小波变换；边缘提取；数学建模
中图分类号：TG444.73 文献标识码：A 文章编号：0253－360X(2008)12－0029－04

0 序 言

快速成形，又叫层制造、直接制造、免实体成形制造、数字制造或电子制造等[1]，该技术尤其适用于小批量零件生产和根据用户定制的大批量零件生产，被认为是先进制造中最具活力和发展潜力的研究方向之一。基于 MAG (metal active gas)焊接的金属零件快速成形技术因具有设备简单、生产效率高、可控参数多、成形致密、力学性能良好等优点而成为低成本金属零件快速成形的研究热点[2－7]，其实质是采用焊接电弧作为热源，由金属材料熔化形成的焊缝逐层堆积而实现金属零件的快速成形，因此，也叫全焊缝制造工艺[1,8]。同普通 MAG 连接工艺相比，MAG 焊接成形不仅需要更好的焊接稳定性、较小的飞溅，而且还需要较低的热输入以及良好的焊缝成形等。为确定焊缝间的最优搭接系数、合理规划焊接成形路径、提高焊接快速成形零件的控形精度，必须对 MAG 焊接成形中的典型单道焊缝截面形态进行精确数学建模。

小波分析是近年来迅速发展起来的用于数字信号处理的新兴学科。小波变换具有良好的时频局部性能和多尺度分析的特性，能将信号在时频空间有效的分解，并能有效提炼出有用信息等优点，已广泛应用于信号处理、图像处理、语音分析、模式识别和量子物理等众多领域中[9－11]。

文中为克服接触式测量方法存在的效率低、精度差等不足，基于小波变换模极大原理对 MAG 快速成形典型焊缝的断面图像进行了焊缝轮廓边缘检测，并对提取的焊缝断面轮廓进行了插值和拟合，建立了焊缝截面数学模型，为实现 MAG 快速成形的数字化精确控形奠定了基础。

1 小波变换模极大边缘检测原理

设 $f(u, v)$ 表示一幅连续图像，其梯度矢量为

$$\nabla f = \left(\frac{\partial f}{\partial u}, \frac{\partial f}{\partial v}\right) \tag{1}$$

该梯度矢量表示 $f(u, v)$ 在点 (u, v) 的最大变化方向。设 (u_1, v_1) 是图像上一点，如果 f 的梯度矢量的模 $|\nabla f| = \sqrt{\left|\frac{\partial f}{\partial u}\right|^2 + \left|\frac{\partial f}{\partial v}\right|^2}$ 在点 (u_1, v_1) 沿着最大变化方向的一维邻域 $(u, v) = (u_1 + v_1) + \lambda \nabla f(u_1 + v_1)$ 中变化，当 $|\lambda|$ 充分小时，在该点取得局部最大值，则称 (u_1, v_1) 是 f 的一个边缘点。

在二维信号的多尺度边界提取中，其小波变换模极大与图像边缘点之间的关系推导如下。

设二维平滑函数 $\theta(u, v)$ 满足

$$\theta(u, v) \geqslant 0 \tag{2}$$

$$\iint_{R^2} \theta(u, v)\mathrm{d}u\mathrm{d}v = 1 \tag{3}$$

$$\lim_{u, v \to \pm\infty} \theta(u, v) = 0 \tag{4}$$

记为

收稿日期：2008－05－08
基金项目：军队科研资助项目（2008WG16），（9140C8502050806）、（9140A27030308JB3502）；中国机械工程学会创新思路预研经费资助项目

$$\theta_s(u,v)=\frac{1}{s^2}\theta\left(\frac{u}{s},\frac{v}{s}\right) \tag{5}$$

则对任意的 $f(u,v)\in L^2(R^2)$，$(f*\theta_s)(u,v)$ 表示 $f(u,v)$ 经 $\theta_s(u,v)$ 平滑后的图像，其中 $s>0$ 为平滑尺度。由 $\theta(u,v)$ 定义两个二维小波，分别为

$$\Psi^1(u,v)=\frac{\partial\theta(u,v)}{\partial u} \tag{6}$$

$$\Psi^2(u,v)=\frac{\partial\theta(u,v)}{\partial v} \tag{7}$$

记

$$\Psi^1_s(u,v)=\frac{1}{s^2}\Psi^1\left(\frac{u}{s},\frac{v}{s}\right) \tag{8}$$

$$\Psi^2_s(u,v)=\frac{1}{s^2}\Psi^2\left(\frac{u}{s},\frac{v}{s}\right) \tag{9}$$

则 $f(u,v)$ 在尺度 s 上的二维小波变换包括两个分量，即

$$W^1_{f(s,u,v)}=(f*\Psi^1_s)(u,v)=\iint_{R^2}f(x,y)\frac{1}{s}\Psi^1\left(\frac{x-u}{s},\frac{y-v}{s}\right)\mathrm{d}x\mathrm{d}y \tag{10}$$

$$W^2_{f(s,u,v)}=(f*\Psi^2_s)(u,v)=\iint_{R^2}f(x,y)\frac{1}{s}\Psi^2\left(\frac{x-u}{s},\frac{y-v}{s}\right)\mathrm{d}x\mathrm{d}y \tag{11}$$

式中：W^1 和 W^2 分别表示二维小波变换的两个分量；$\Psi^k_s(u,v)=\frac{1}{s^2}\Psi^k_s(-u,-v)$，$k=1,2$。

可以证明

$$\begin{Bmatrix}W^1_{f(s,u,v)}\\W^2_{f(s,u,v)}\end{Bmatrix}=s\begin{Bmatrix}(f*\Psi^1_s)(u,v)\\(f*\Psi^2_s)(u,v)\end{Bmatrix}=s\begin{Bmatrix}\dfrac{\partial((f*\theta_s)(u,v))}{\partial u}\\\dfrac{\partial((f*\theta_s)(u,v))}{\partial v}\end{Bmatrix}=s\nabla(f*\theta_s)(u,v) \tag{12}$$

因而，$(f*\theta_s)(u,v)$ 梯度矢量 $\nabla(f*\theta_s)(u,v)$ 的模与式(13)小波变换的模(用 M 表示)成比例，即

$$M_{f(s,u,v)}=\sqrt{|W^1_{f(s,u,v)}|^2+|W^2_{f(s,u,v)}|^2} \tag{13}$$

梯度方向与水平方向 u 的相角(用 A 表示)为

$$A_{f(s,u,v)}=\arctan\left(\frac{W^2_{f(s,u,v)}}{W^1_{f(s,u,v)}}\right) \tag{14}$$

因此，计算一个平滑函数 $(f*\theta_s)(u,v)$ 沿着梯度方向的模极大值等价于计算小波变换的模极大值，即

$$\bar{n}_j(u,v)=(\cos A_{f(2^j,u,v)},\sin A_{f(2^j,u,v)}) \tag{15}$$

则单位矢量 $\bar{n}_j(u,v)$ 与梯度矢量 $\nabla(f*\theta_s)(u,v)$ 是平行的。因此，在尺度 s 下，若模 $M_{f(s,u,v)}$ 在点 (u_1,v_1) 沿着 $(u,v)=(u_1+v_1)+\lambda\nabla f(u_1+v_1)$，当 $|\lambda|$ 充分小时取到局部极小值，则点 (u_1,v_1) 就是 $(f*\theta_s)(u,v)$ 的一个边缘点，从而是 $f(u,v)$ 的一个突变点，而边界的方向与 $\bar{n}_j(u,v)$ 垂直[12]。这表明，通过检测二维小波变换的模极大点可以确定图像的边缘点。沿着边界方向将任意尺度下的边缘点连接起来就可形成该尺度下沿着边界的模极大曲线。

2 焊缝轮廓图像处理结果及分析

2.1 试验条件

焊接成形设备主要由 ABB IRB2400/16 机器人(瑞典产)和 Fronius 全数字 Trans Puls Synergic 4000 型脉冲 MAG 焊机(奥地利产)组成。试验用基材为中碳钢，试样被切割成 100 mm×100 mm×12 mm 的方形试块，采用铣削加工除掉试样表面的杂物和氧化物。焊接保护气体为氩气 80%，二氧化碳 20%，焊丝材料为 H08Mn2Si。焊接工艺参数如表 1 所示，其它工艺参数保持不变。

表 1 焊接工艺参数

Table 1 Welding parameters

焊接电流 I/A	电弧电压 U/V	焊接速度 v/(mm·s^{-1})	气体流量 q/(L·min^{-1})
115	28	25	12

2.2 焊缝截面边缘提取

焊缝截面边缘提取过程如下。

(1) 加载焊缝截面图像。

图 1 为焊缝的截面轮廓。从图中可以看出，该焊接工艺下成形较为稳定、规则，并且飞溅较小。将该图像加载到小波变换程序中。

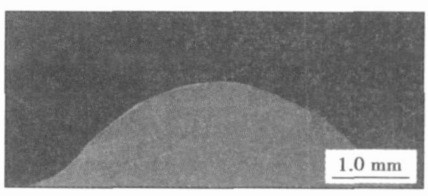

图 1 MAG 快速成形焊缝截面轮廓

Fig. 1 Welded bead cross-section of rapid prototyping by MAG

(2) 在尺度 $s=2^j$ 下，进行焊缝轮廓的二维小波变换计算。

(3) 计算每一点的模值和相角 $A_{f(2^j,u,v)}$ 的正切值。

对每个像素点 (n,m)，计算

$$M_{f(s,u,v)}=\sqrt{|W^1_{f(s,u,v)}|^2+|W^2_{f(s,u,v)}|^2} \tag{16}$$

$$\tan A_{f(s,u,v)} = \frac{W^2_{f(s,u,v)}}{W^1_{f(s,u,v)}} \tag{17}$$

(4) 求边界点。

确定阈值 $T > 0$，对 n，$m = 0, 1 \cdots, n-1$，如果 $M_{f(s,u,v)} \geqslant T$，且 $M_{f(s,u,v)}$ 取得局部极大值，即 (n, m) 为模极大点，则 (n, m) 就是一个边界点。

(5) 在各个尺度上连接边界点，形成各尺度下沿着边界的极大曲线。

图 2 为焊缝截面轮廓经上述各步骤处理后的边缘提取结果图。可以看出，采用小波变换提取的焊缝截面轮廓较为清晰。

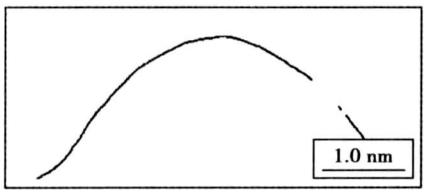

图 2　小波变换提取的焊缝截面边缘

Fig. 2　Edge detection by wavelet transform

2.3　焊缝轮廓边缘插值

为了实现对焊缝轮廓的精确建模，分别采用二次 B 样条曲线，三次样条曲线以及带约束的三次样条曲线进行插值。图 3 给出了不同插值方法的插值结果。从图 3a，b 可以看出，采用二次 B 样条曲线和三次样条曲线插值时，在轮廓断续点出现了局部突变，而采用带约束的三次样条曲线插值结果（图 3c）则呈平滑、连续过渡，这是由于带约束的三次样条曲线其一、二阶导数为连续函数所致。因而采用带约束的三次样条曲线插值结果作为焊缝轮廓的实际数据进行后续处理。

2.4　焊缝模型建立

采用了 Levenberg-Marqurdt 算法进行了 10 次迭代运算对焊缝截面轮廓进行了拟合。Levenberg-Marqurdt 是一种通过在 Hessian 矩阵上加一个正定矩阵来分析处理的优良非线性最小二乘优化方法，该方法最初由 Levenberg 和 Marqurdt 提出来的，故称为 Levenberg-Marqurdt 方法。拟合出的焊缝截面数学模型为

$$y = 1.40\sin(2\pi x/8.32 + 6.23) \tag{18}$$

图 4 和图 5 分别给出了置信度为 99.99% 条件下采用正弦曲线拟合的结果和残差分布结果，虚线表示正弦曲线，粗实线表示焊缝轮廓的实际数据。可以看出，采用正弦函数来拟合焊缝截面轮廓时，其理论值与实际值几乎完全重合。同时，拟合残差呈随机性分布，差值在 ±0.08 mm 范围内，表明采用正弦函数拟合时具有较小的误差和较高的精度，因此

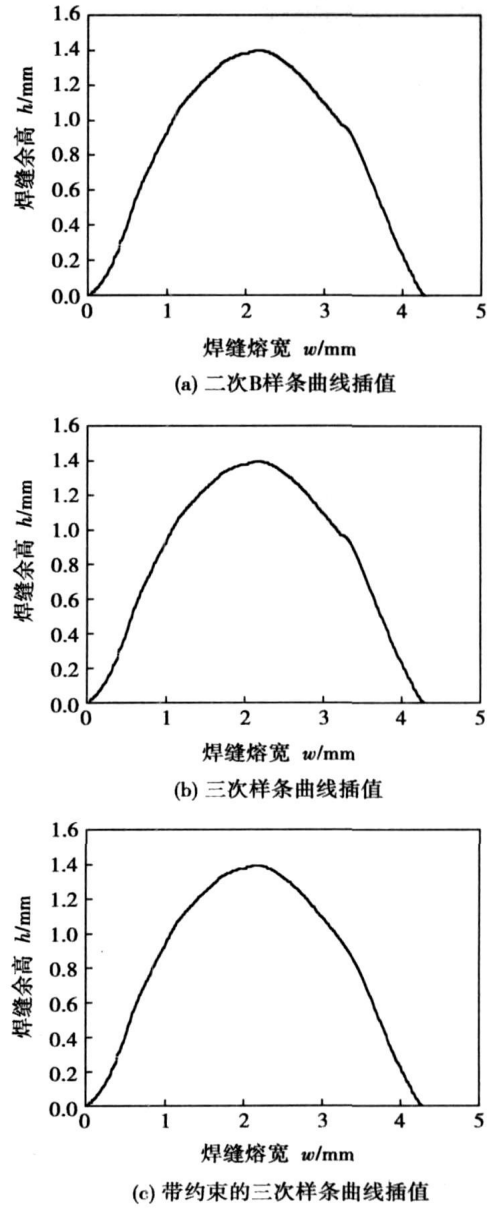

图 3　不同插值方法的插值结果

Fig. 3　Results with different interpolation methods

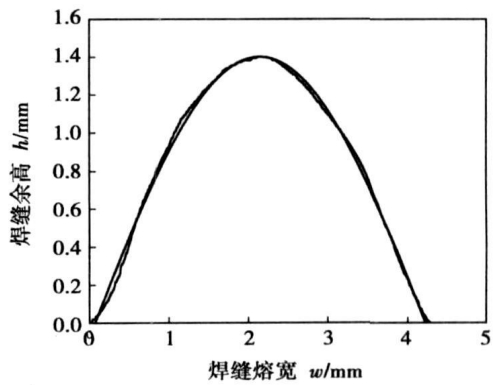

图 4　焊缝截面轮廓拟合结果

Fig. 4　Curve fitting of weld seam profile with sine curve

采用正弦函数作为焊缝截面轮廓模型是科学、合理的。

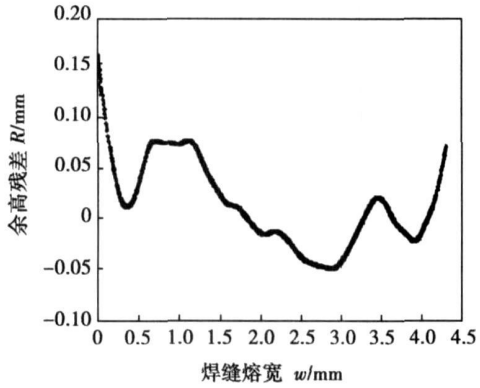

图 5 拟合残差分布结果

Fig. 5 Residuals distribution of fitting function

3 结 论

(1) 采用小波变换模极大法来提取焊缝截面轮廓是可行的,提取出的焊缝截面轮廓图像较为清晰。

(2) 采用不同插值方法对轮廓提取中的局部断续插值结果表明,带约束的三次样条曲线同二次 B 样条曲线和三次样条曲线相比,过渡更为连续、平滑。

(3) 该试验条件下得到的单道焊缝截面轮廓数学模型为正弦曲线。

参考文献:

[1] Wang H, Jiang W, Ouyang J, *et al*. Rapid prototyping of 4043 Al-alloy parts by VP-GTAW [J]. Journal of Materials Processing Technology, 2004, 148(1): 93−102.

[2] Yin Y, Hu S, Zhang X, *et al*. Effect of processing parameters on figuration during the GMAW rapid prototyping process [J]. China Welding, 2006, 15(4): 30−33.

[3] Male A T, Chen Y W, Pan C, *et al*. Rapid prototyping of metal components by plasma-jet forming [J]. Journal of Materials Processing Technology, 2003, 135(2−3): 340−346.

[4] Terakubo M, Janghwan Oh, Kirihara S, *et al*. Freeform fabrication of titanium metal by 3D micro welding [J]. Materials Science and Engineering A, 2005, 402(1−2): 84−91.

[5] Zhang Y M, Chen Y, Li P, *et al*. Weld deposition-based rapid prototyping: a preliminary study [J]. Journal of Materials Processing Technology, 2003, 135(2−3): 347−357.

[6] Song Y A, Park S, Choi D, *et al*. 3D welding and milling: Part I—a direct approach for freeform fabrication of metallic prototypes [J]. International Journal of Machine Tools &Manufacture, 2005, 45(9): 1057−1062.

[7] Song Y A, Park S, Chae S W. 3D welding and milling: part II—optimization of the 3D welding process using an experimental design approach [J]. International Journal of Machine Tools & Manufacture, 2005, 45(9): 1063−1069.

[8] 史耀武. 成型焊接快速零件制造技术的发展[J]. 中国机械工程, 1994, 5(6): 1−2.

[9] Pajares G. A wavelet-based image fusion tutorial [J]. Pattern Recognition, 2004, 37(9): 1855−1872.

[10] Ellinas J N, Sangriotis M S. Stereo image compression using wavelet domain vector hidden Markov tree model[J]. Pattern Recognition 2004, 37(7): 315−1324.

[11] 张德丰, 张葡青. 基于小波的图像边缘检测算法研究[J]. 中山大学学报(自然科学版), 2007, 146(3): 39−42.

[12] 孙延奎. 小波分析及应用[M]. 北京: 机械工业出版社, 2005.

作者简介: 曹 勇, 男, 1974 年出生, 博士研究生, 讲师。主要从事机器人焊接快速成形及修复中的控形与控性研究工作。发表论文 2 篇。

Email: COYG74@live.cn

[上接第 4 页]

参考文献:

[1] 张瑞华, 樊 丁. 不锈钢 A-TIG 活性剂的焊接性研究[J]. 甘肃工业大学学报, 2002, 28(2): 12−14.

[2] 张瑞华, 樊 丁. 低碳钢 A-TIG 活性剂的焊接性[J]. 焊接学报, 2003, 24(1): 85−87.

[3] Howse D S, Lucas W. Investigation into arc constriction by active fluxes for tungsten inert gas welding [J]. Science and Technology of Welding and Joining, 2000, 5(3): 18−193.

[4] Marya M, Edwards G R. Chloride contributions in flux-assisted GTA welding of magnesium alloys [J]. Welding Research, 2002(11): 291−298.

[5] Fujii H, Lu S P, Nogi K, *et al*. Welding pool convection under microgravity and effect of Marangoni convection on weld shape[C]// Proceedings of IFWT in aviation and space industries, Beijing: China Machine Press, 2004: 75−87.

[6] 刘凤尧, 杨春利, 林三宝, 等. 活性化 TIG 焊熔深增加机理的研究[J]. 金属学报, 2003, 39(6): 661−665.

[7] Takamichi I, Roderick I L. 液态金属的物理性能[M]. 北京: 科学出版社, 2006.

[8] Heiple C R, Roper J R, Stanger R T, *et al*. Surface active element effects on the shape of GTA, laser and electron beam welds [J]. Welding Research Supplement, 1983, (3): 72−77.

作者简介: 樊 丁, 男, 1961 年出生, 教授, 博士研究生导师。主要从事焊接物理、焊接智能控制以及激光加工等方面的研究工作。发表论文 140 余篇。

Email: fand@lut.cn

versity, Tianjin 300072, China). p17—19, 24

Abstract: Arc spraying and plasma cladding process was used to prepare the aluminum composite coating. The microstructure and phase structures of the clad alloy layer and the interface of alloy layer and steel matrix composites were analyzed. The results show that the tight alloy layer without pore and inclusion is obtained, and the coating and the steel are metallurgically compacted. The clad alloy layer consists of phase Fe_3Al, FeAl, α-Fe and Al_2O_3. Microhardness of the clad alloying layer will be 514 HV.

Key words: plasma cladding; Fe_3Al; intermetallic compound

Application of pre-scanning technology with laser to seam-curved tracking XIAO Zengwen, LIU Jifeng, CHEN Zhichao, GONG Xun (Department of Mechanical Engineering, Nanjing Institute of Technology, Nanjing 211167, China). p20—24

Abstract: The structured-light technology of traditional seam tracking makes front guiding error great if the curvature is varying. To solve the problem, a structured-light pre-scanning technology with double lines is produced. The seam is scanned before welding along the planned track of the robot. A laser line is added under the welding torch tip to indicate the front guiding error that will be recorded on time sequence and be eliminated when welding. A seam tracking system and its mathematical model are established. An image processing system is advanced, which the integrations of image processing technologies including median filtering, threshold transforming, thinness transforming and subsection beeline fitting locate the seam middle exactly. Tests show that the technology combined with the image processing system has the characteristics of strong anti-jamming, little error and fast processing speed, and it can meet the request of real time tracking.

Key words: seam tracking; structured-light; pre-scanning; image process; curved seam

Microstructure and shear strength of diffusion brazed Al_2O_3-TiC/Q235 joint WANG Juan[1], LI Yajiang[1], S. A. GERASIMOV[2] (1. Key Laboratory of Liquid Structure and Heredity of Materials, Shandong University, Jinan 250061, China; 2. Materials Science Department, Bauman Moscow State Technical University, Moscow 105005, Russia). p25—28

Abstract: An Al_2O_3-TiC/Q235 joint, Al_2O_3-TiC ceramic composite with steel Q235, was obtained by diffusion brazing in vacuum, using a combination of Ti and Cu as multi-interlayer. The interfacial strength was measured by shear testing and the result was explained by the fracture morphology. Microstructure of the Al_2O_3-TiC/Q235 joint was investigated by scanning electron microscope (SEM), energy-dispersion spectroscopy (EDS) and X-ray diffraction (XRD). The results indicate that the Al_2O_3-TiC/Q235 joint with a shear strength of 122 MPa can be obtained by controlling heating temperature at 1 110 ℃, multi-interlayer Ti/Cu/Ti is fused fully and diffused reaction to produce an obvious interfacial transition zone with a thickness of about 80 μm, and there are Ti_3AlC_2, Fe_2Ti, Cu and TiC in the transition zone.

Key words: Al_2O_3-TiC; diffusion brazing; shear strength; microstructure

Cross-section modeling of weld bead for rapid prototyping by MAG welding based on wavelet transform CAO Yong, ZHU Sheng, SUN Lei, SHEN Canduo, LIANG Yuanyuan, WANG Wanglong (National Defense Key Laboratory for Remanufacturing, Academy of Armored Forces Engineering, Beijing 100072, China). p29—32

Abstract: A new modeling method of weld bead profile by MAG welding process was proposed and the edge of the profile was extracted based on wavelet transform. The different interpolation methods, the cubic spline, the constrained cubic spline and the B-spline curve, were utilized respectively, the cross-section edge of weld bead was fitted by least square method, and then the mathematical model of the profile was achieved. The experimental results show that the method is effective to detect the cross-section outline of the profile, the constrained cubic interpolation is preferred choice to interpolate the data of the profile, and the cross-section profile mathematical model of weld bead is sine curve under our experiments.

Key words: rapid prototyping; wavelet transform; edge detection; modeling

Microstructure and wear resistance of plasma cladding Al_2O_3+TiO_2/Fe alloy composite coating LU Jinbin, LIANG Cun, PENG Zhuqin, ZHANG Zhaojun (College of Material and Chemical Engineering, Zhongyuan University of Technology, Zhengzhou 450007, China). p33—36

Abstract: Plasma cladding Ni-Cr-B-Si-Fe-based alloy coating and Fe-based alloy composite coating with Al_2O_3+TiO_2 were obtained on the Q235 substrate, and microstructure, microhardness and wear resistance of the two coatings were investigated contrastively. The results show that the interface solidification form of Fe-based alloy composite coating with Al_2O_3+TiO_2 have changed. They become small dendrite from primary lathy dendrite, and offer core for solidification. The microstructure is mainly based on γ-Fe with fine particles, and its microhardness can reach 600~655 HV0.2.

Key words: plasma cladding; microhardness; wear resistance; Al_2O_3+TiO_2

Data collecting system of pipe arc acoustic emission characteristics LIU Lijun[1,2], LAN Hu[1], DUAN Hongwei, WEN Jianli[1] (1. School of Material Science & Engineering, Harbin University of Science and Technology, Harbin 150080, China; 2. Ningbo Institute of Technology, Zhejiang University, Ningbo 315100, China). p37—40

Abstract: As the arc sound signal contains plenty of welding information which is an important source signal for welding quality control, arc acoustic emission signal (AAES) propagated in pipeline structure is low-noise, and AAES collecting system is designed for pipe TIG welding. The hardware system consists of sensor, signal adaptor circuit, data collecting card and industrial workstation. Based on virtual instrument programming software (LabVIEW), the high speed AAES collecting software system is designed by means of triggering interrupt, packaging function modules and calling dynamic